1150 hp motor design, electromagnetic and thermal analysis

Qasim Al'Akayshee [1], and David A Staton [2]

[1]Mawdsley's Ltd., The Perry Centre, Davey Close,
Waterwells, Gloucester GL2 4AD
phone: +44 1452 888311 – fax: +44 1452 888309 – e-mail: qasim@mawdsleys.com

[2]Motor Design Ltd.
1 Eaton Court, Tetchill, Ellesmere, Shropshire SY12 9DA
phone: +44 1691 623305 – fax: +1 419 831 9255 – e-mail: dave.staton@motor-design.com

***Abstract* – This paper describes the electromagnetic and thermal design of 1150 hp vector controlled induction motor. The system replaces an old dc drilling motor in an oil field application. The systems performance is calculated using a conventional equivalent circuit - the parameters of which are calculated using an analytical electromagnetic design package. This is used iteratively with a lumped circuit thermal model to optimise both aspects of the design. Two-dimensional electromagnetic finite element analysis is then used to fine tune the design. The work is validated by experimental results.**

1. Introduction

The paper describes the design and testing of an induction motor for the oil field drilling application. The system replaces an old DC machine. The machine is driven from an IGBT inverter using AC vector control. A photograph of the new motor is shown in Fig. 1.

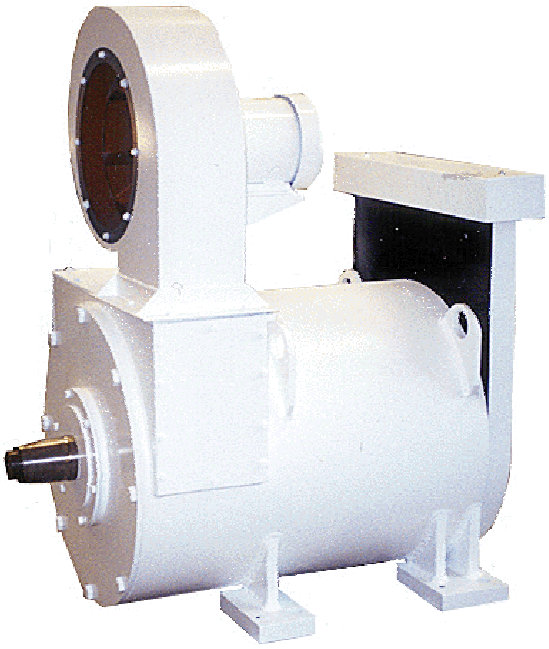

Fig.1. showing the AC vector control motor

2. The Drive Motor

The motor is designed to produce 1150 hp continuously – so that is can provide the required continues drilling torque of 7690 lb.ft. The system employs two inverters to give redundancy and standby capability.

The machine has 6 poles. The double layer 10/12-corded winding is accommodated in 72 slots. The stator laminations are made from Losil material. Class H inverter grade wire is used so as to withstand the sharp impulse repetitive waveforms produced from the switching process at high frequencies.

A stator view of the motor is shown in Fig. 2. The forced air blower cooling system is designed to pass air through axial ducts on both the stator and rotor. The stator ducts comprise of gaps between stator lamination and the housing. The rotor lamination has 20 x 30 mm diameter holes along the rotor core length. The axial ducts are clearly seen in Fig 7.

Fig.2. showing the stator pack and the winding

3. Design Strategy

Fig 3 shows the basic flow diagram of the design strategy used. In the early stages of the design process there is strong iteration between the electromagnetic equivalent circuit and lumped circuit thermal design algorithms. As both the

electromagnetic and thermal packages used are based on analytical algorithms they give near instantaneous calculation speeds and enable many design ideas to be investigated in a short period of time. The aim is to try to optimise the overall design. Both the electromagnetic and thermal design need to be considered at the same time as they are not interdependent – the losses being dependent upon the temperature and the temperature on the losses. Electromagnetic finite element is used to check and fine tune designs identified as being viable using the analytical tools. Again some iteration is necessary in order to achieve the optimum solution. An additional benefit of carrying out finite element analysis is that the analytical formulations used in the sizing stages can be fine tuned to give more reliable results for future designs.

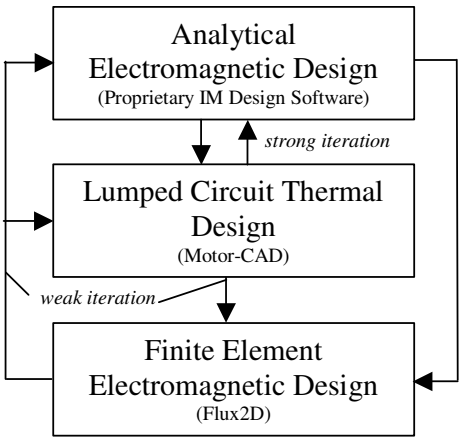

Fig.3. Design flow diagram

4. Equivalent circuit and practical results

A conventional equivalent circuit calculation method is used to calculate the performance of the machine [1], [2]. The machines produces constant torque up to 800 rpm and constant power above this speed. Fig. 4 shows the calculated and measured machine characteristics. In addition to the full load torque and power values, maximum ratings are also shown. The overload requirements are 157% full load power for at least 2 minutes with a 257% peak power.

The machine has been tested operating from an 900V dc link inverter. During the test the motor is coupled to two DC generators, one on each side of the shaft as shown in Fig.5. Fig. 6 shows the measured saturation levels. Table I shows a comparison between the calculated and measured performance.

TABLE I
Test and calculated machine parameters

Machine parameters	Calculated	Measured
Line curren(amps)	1039	1050
Power factor	0.87	0.82
Shaft torque(Ib.ft)	7689	7550
Shaft speed (rpm)	789	782
Effeciency (%)	95.6	94.2

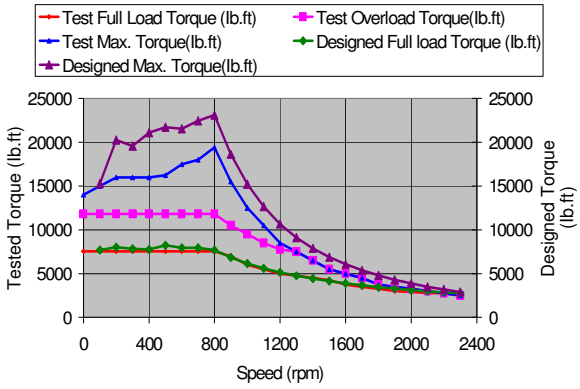

Fig.4. Measured and calculated performance

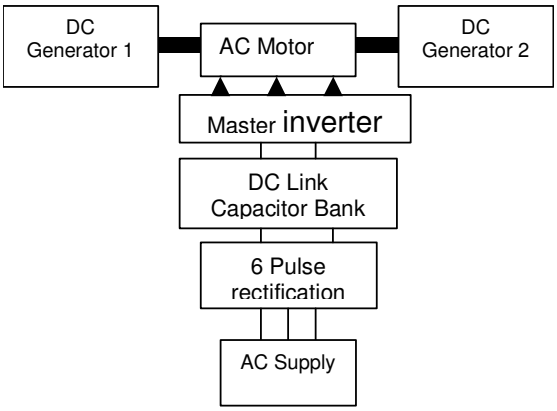

Fig.5. Experimental motor set up

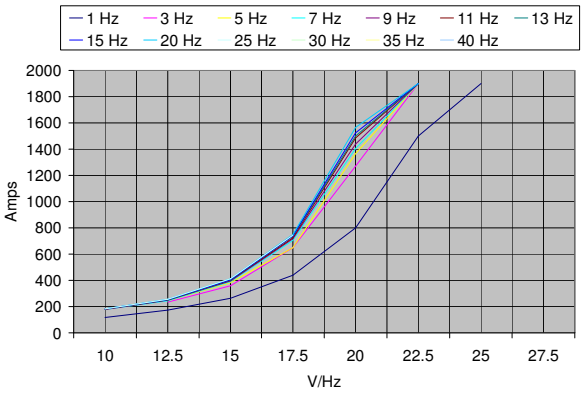

Fig.6. Saturation curves

5. Thermal Analysis

Use was made of a commercially available thermal lumped circuit program specifically developed for the thermal analysis of electrical motors and generators [3]. The motors geometry is input into the software as shown in Fig. 7 and Fig. 8. Both the radial and axial cross sections of the motor must be described as unlike the electromagnetic analysis the thermal circuit is truly 3-dimensional in nature.

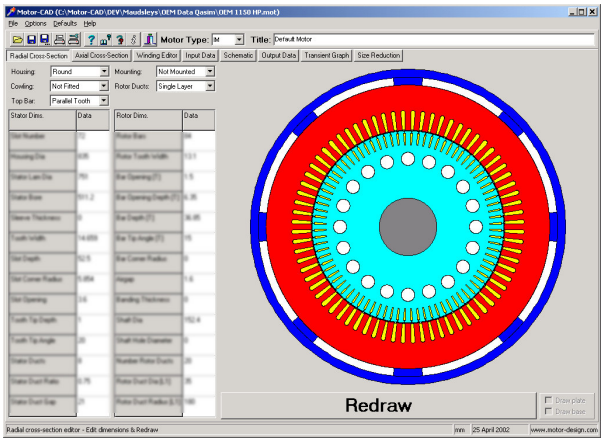

Fig.7. Motor radial cross-section

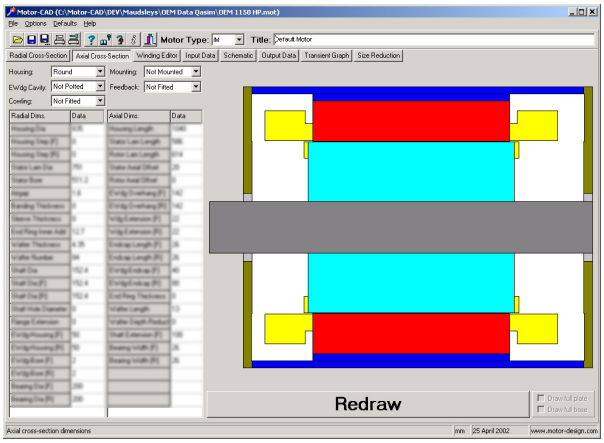

Fig.8. Motor axial cross-section

It is not practical to model each individual conductor so the slot-liner/copper/insulation layered winding model illustrated in Fig. 9. is used. This enables the prediction of winding hotspots in the centre of the coil and the estimation of the short time constant associated with the winding rather than that of the whole motor. The number of layers and copper to insulation thickness ratio is set by the wire diameter, number of turns and subsequent slot-fill. The winding diagrams are useful for gaining a visual indication of the slot-fill which can be achieved.

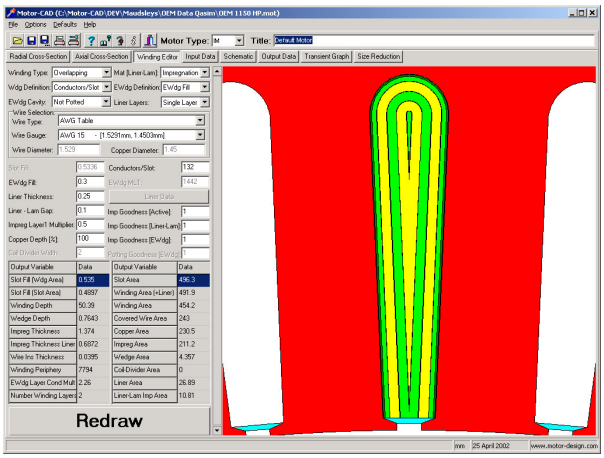

Fig.9. Winding layered thermal model

Thermal resistance values for all conduction paths within the motor are calculated automatically from motor dimensions and material data. Convection and radiation are also automatically accounted for in the calculation. Radiation is just dependent upon the emissivity of the exposed surfaces. Convection is calculated from proven laminar and turbulent convection correlations [4]. For instance the convective cooling for the ducts is based on the dimensionless enclosed channel correlations detailed in [4], [5], and [6].

Local air velocity is required in order to calculate the local convective heat transfer. This is calculated by solving a separate network of flow resistances. A flow resistance depends upon the fluid friction at the wall surface and changes in flow condition – such as expansions and contractions in the flow circuit and restrictions due to obstructions in the flow path. The changes in flow condition typically predominate in electrical machines as the flow path is relatively short. Fig. 10. shows the intersection of the fan (blower) characteristic and system flow resistance characteristic for the motor being considered here. The resulting total volume flow rate is 3300CFM. Temperature and power flow predictions within the motor are shown in the schematic diagram shown in Fig. 11. Excellent agreement with test was achieved, the measured winding hot spot being 157C and the calculated value being 161C – when cooled by 3300CFM from the external blower.

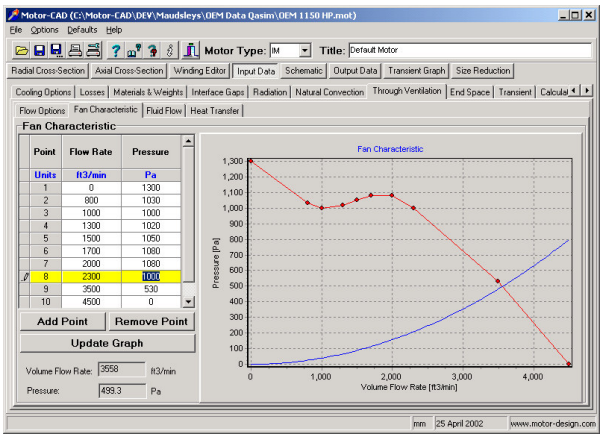

Fig.10. Blower fan and system characteristics

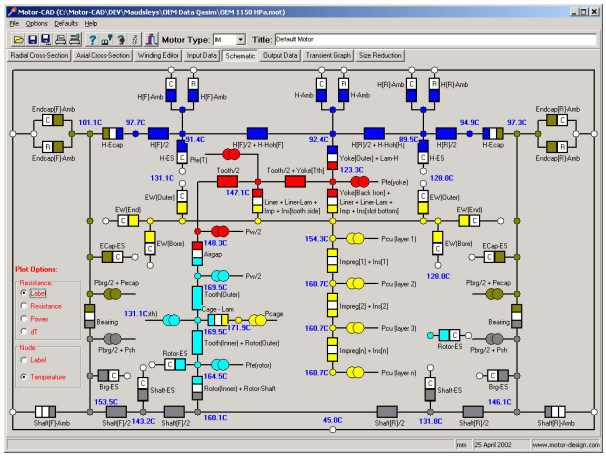

Fig.11. Thermal schematic showing steady-state

6. Electromagnetic Finite Element Analysis

The commercially available Flux2d package [7] has been used to perform the finite element analysis shown in this paper. A key feature of the software are the ability to carry out combined electromagnetic and circuit analysis. The software uses a solid conductor model to model the squirrel cage. The external circuit used in this instance is shown in Fig. 12. Fig. 13 and Fig. 14 show the full load flux and flux density plots for the motor. The six poles arrangement is clearly shown.

Finite element analysis has been used to confirm the performance before production and to fine tune the design. It has also been found useful for improving the analytical algorithms used in the initial stages of the design, so enabling shorter and more accurate future design cycles. Calculated performance results at operating points around the rated point are given in Tables II and III – these compare well with measured data.

TABLE II
FEA Results

Speed [rpm]	Btooth [T]	Byoke [T]	Brotor [T]
790.86	1.88	1.55	1.82
790	1.89	1.55	1.82
789	1.90	1.55	1.82
788	1.90	1.55	1.82

TABLE III
FEA Results

Speed [rpm]	Slip	T [Nm]	Irms [A]	Pf	Psft [kW]
790.86	0.01143	8996	919	0.837	745
790	0.0125	9753	988	0.846	807
789	0.01375	10615	1069	0.852	877
788	0.015	11452	1150	0.857	945

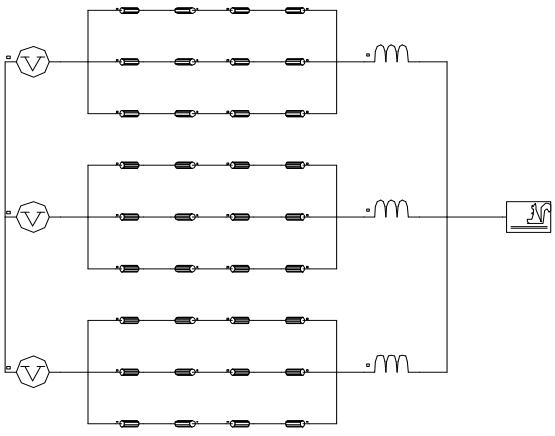

Fig.12. Circuit used in FEA analysis

7. Conclusion

Six machines of the type described in the paper are now in service and are performing very satisfactory. The machine design shows a high rotor flux density – but this has been found acceptable as the motors are operated from an inverter giving a controlled rotor frequency (slip frequency). The rotor iron loss at the tooth tips is probably a little high as these see the air gap field harmonics due to the stator slotting. Table V shows the calculated and the finite element flux densities in the motor are in relatively good agreement considering the required simplifications in the analytical design algorithms. The good thing is that the analytical algorithms are being continually improved by FEA feedback.

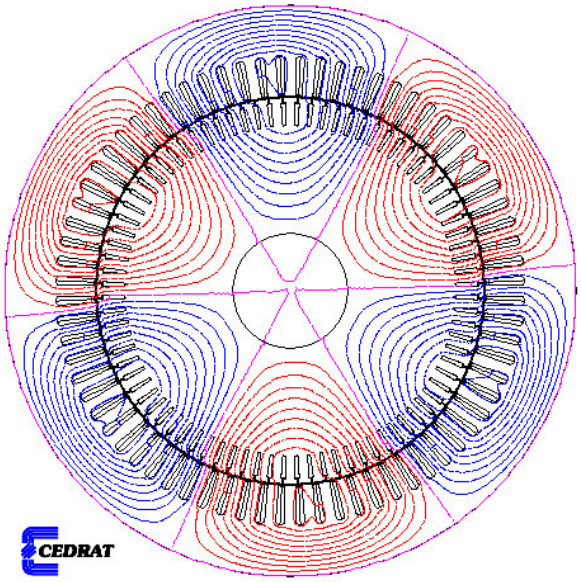

Fig.13. FEA flux plot (rated condition)

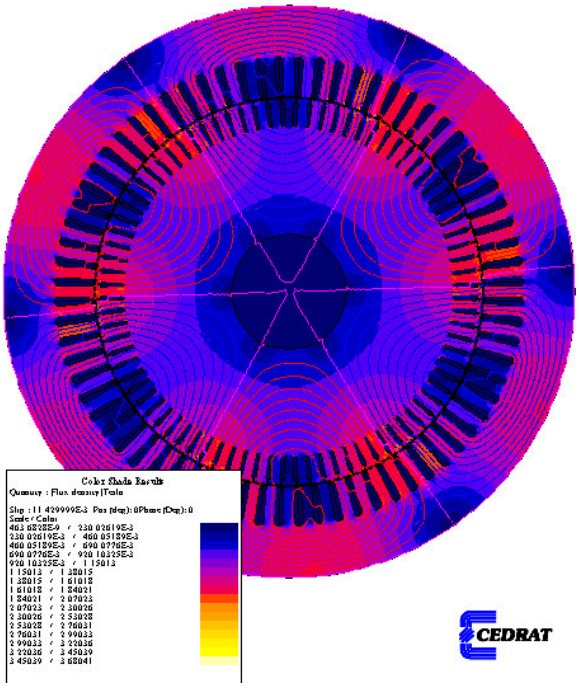

Fig.14. FEA flux density plot (rated condition)

TABLE V
Comparison between equivalent circuit based calculation and FE of flux density within the machine

Flux density (T)	Calculated	FE Modelling
Stator core	1.62	1.55
Stator teeth	1.73	1.88
Rotor core	1.13	1.55
Rotor teeth (body)	1.76	1.88
Rotor teeth (tip)	1.71	1.82
Air gap	1.13	1.18

References

[1] AC_IND – A DATAFLEX Program for the design of AC induction motors, May 1992, Mawdsley's Ltd., The Perry Centre, Davey Close, Waterwells, Gloucester GL2 4AD.

[2] PERF – A DATAFLEX Program for calculating the performance of AC induction motors, May 1992, Mawdsley's Ltd., The Perry Centre, Davey Close, Waterwells, Gloucester GL2 4AD.

[3] Motor-CAD software – www.motor-design.com

[4] Mills, A.F., Heat Transfer, Prentice Hall, 1999

[5] Edwards, D.K., Denny, V.E., Mills, A.F. : Transfer Processes, 2nd ed., Hemisphere, Washington, D.C. (1979)

[6] Gnielinski, V.: 'New equations for heat and mass transfer in turbulent pipe and channel flow', Int. Chemical Engineering, 16, pp.359-368 (1976)

[7] Flux2D software – www.cedrat.com